한국에너지공학회지(1993), 제2권 제1호
Energy Engg. J (1993), Vol. 2, No. 1 pp. 114~122

Effects of Catalyst Pore Structure on Reactivity in Simplified Reaction System

Young Woo Rhee and Jae Ek Son
Energy & Environmental Research Department, Korea Institute of Energy Research, 71-2, Jang-dong, Yoosung-gu, Daejeon, Korea

Abstract—A model describing the reaction rate and catalyst deactivation in a simplified reaction system was developed to investigate the significance of catalyst pore structure in terms of porosities, porosity ratios, and size ratios of reactant to pores. The model showed that the unimodal catalyst could give a better performance than the bimodal in certain circumstances and the crossover found in the reactivity curves resulted from a trade-off between surface area and diffusivity. Under the assumption of uniform coke buildup, the bimodal catalyst appeared to provide better resistance to deactation than unimodal catalyst.

1. Introduction

The intraparticle diffusional limitation that is known to be a detrimental factor to the catalyst activity has been widely reported in the reactions of such large reactants as coal and asphaltenes.[1-9] The influence of this hindered diffusion might be alleviated by modifying the catalyst pore structure. Namely, the concept of a bimodal catalyst consisting of macro and micropore system can be applied to allow greatly improved accessibility of large molecules. The large macropores serve as diffusing channels for large reactant molecules in order to gain easy access to the interior of the pellet, while the micropores enclosing each channel provide sufficient surface area for reaction. The bimodal catalyst has reasonable theoretical background for improving the catalyst activity and prolonging the catalyst life since the reaction rate constant is generally expressed in terms of effective diffusivity and catalytic surface area. The macropores will mainly contribute to enhancing the effective diffusivity of the catalyst, thereby preventing a rapid pore plugging during the catalyst deactivation, while the micropores mainly contribute to the catalytic surface area.

Although some commercial catalysts such as Shell-317, Amocat-1A, and Amocat-1C are bimodal, their applicability to, especially, coal liquefaction is still unclear. The performances of these bimodal catalysts seem to strongly depend on the reaction systems and do not always give improved results compared to the unimodal catalysts. Also it is difficult to compare the performance of bimodal catalysts with that of unimodal catalysts since the catalysts have, in most cases, different manufacturing procedures where many unknown factors are involved.[10-11]

In this study, the effects of introducing macropores to catalyst pore geometry on the reactivity have been investigated by developing a simplified model based on the work of Rhee and Guin.[12] The model used the simplest form of bimodal pore distribution, i.e. two Dirac delta functions of macro- and micropores and was applied to assess the effects of porosities and size ratios of reactant to pores.

2. Model Development

2-1. Reaction Rate.

Pellet catalysts are assumed to have the simplest bimodal pore size distribution, i.e. two δ-functions. for a bimodal pore size distribution let $g(A)=N_1\delta(A-A_1)+N_2\delta(A-A_2)$, where N_1 is the number of pores of area A_1 per unit volume of pellet and N_2 is the number of pores of area A_2 per unit volume of pellet. In this case the two properties ρ_s and ρ_c completely define all other properties such as ε, S_v, S_g. Now, a first order, diffusion controlled reaction is assumed. Thus the

*The author the whom correspondences should be addressed.

reaction rate[12], r_v is

$$r_v = k(S_v D_e)^{1/2} \quad (1)$$

where $k = C_s^s S_x \sqrt{k_s / V_p}$ = constant.

The porosity is defined as $\varepsilon = \varepsilon_1 + \varepsilon_2$, where ε_1 and ε_2 are pore fractions of micro (R_1)- and macro (R_2)-pores.

From the definition,

S_v = surface area of pores/volume of pellet
$= \Sigma$(surface area of pores/volume of pores)$_i$ x(volume of pores/volume of pellet)$_i$
$= \Sigma(2/R_i)(\varepsilon_i)$
$= 2(\varepsilon_1/R_1 + \varepsilon_2/R_2)$ (2)

Introducing dimensionless variables $\lambda_i = R_m/R_i$ where R_m is molecular size (radius),

$$S_v = (2/R_m)(\varepsilon_1 \lambda_1 + \varepsilon_2 \lambda_2) = (2\varepsilon/R_m)[(\varepsilon_1/\varepsilon)\lambda_1 + (\varepsilon_2/\varepsilon)\lambda_2] \quad (3)$$

$$D_e = \Sigma(\varepsilon_i/\tau)(D_m K_{ri} K_{pi}) = (D_m/\tau)(\varepsilon_1 K_{r1} K_{p1} + \varepsilon_2 K_{r2} K_{p2}) = (\varepsilon D_m/\tau)[(\varepsilon_1/\varepsilon) K_{r1} K_{p1} + (\varepsilon_2/\varepsilon) K_{r2} K_{p2}] \quad (4)$$

Equation 4 assumes τ is not a function of pore size. Substituting equations 3 and 4 into equation 1 gives

$$r_v = a(\varepsilon^2 D_m/R_m)^{1/2} [(\lambda_1 \varepsilon_1/\varepsilon + \lambda_2 \varepsilon_2/\varepsilon) \times (\varepsilon_1/\varepsilon K_{r1} K_{p1} + \varepsilon_2/\varepsilon K_{r2} K_{p2})]^{1/2} \quad (5)$$

where a is a constant. For simplicity, a constant molecular size is considered, thus, D_m is constant. Under these assumptions, the reaction rate will be a function of ε, $\varepsilon_2/\varepsilon$ and λ_i as shown in equation 5, that is,

$$r_v = a' \varepsilon [(\lambda_1 \varepsilon_1/\varepsilon + \lambda_2 \varepsilon_2/\varepsilon) \times (\varepsilon_1/\varepsilon K_{r1} K_{p1} + \varepsilon_2/\varepsilon K_{r2} K_{p2})]^{1/2} \quad (6)$$

where a' is a constant and $0 \le \lambda_i \le 1$.

In case of a unimodal catalyst, equation 6 becomes

$$r_v = a' \varepsilon_1 (\lambda_1 K_{r1\ p1})^{1/2} \quad (7)$$

2-2. Catalyst Deactivatin.

In order to investigate the effects of pore plugging on the catalyst activity, an evolution equation for pore size distribution function g(A, t) could be developed. However, if every pore is assumed to be uniformly coated at time t, equation 7 will be applicable uniformly. A uniform coating thickness is defined as δ, which ranges from zero to the initial micropore radius, R_{1o}. Thus, micropore radius R_1 and macropore radius R_2 will be expressed during the activation process as follows:

$$R_1 = R_{1o} - \delta \qquad R_2 = R_{2o} - \delta \quad (8)$$

where $0 \le \delta \le R_{1o}$. A dimensionless parameter DT is defined as $DT = \delta/R_{1o}$, which will range from 0 to 1. The subscript o represents the initial state, i.e. t=0.

The change in λ_i will be

$$\frac{\lambda_1}{\lambda_{1o}} = \frac{R_{1o}}{R_1} = \frac{R_{1o}}{R_{1o} - \delta} = \frac{1}{1 - DT} \quad (9)$$

$$\frac{\lambda_2}{\lambda_{2o}} = \frac{R_{2o}}{R_2} = \frac{R_{2o}}{R_{2o} - \delta} = \frac{1}{1 - (\lambda_{2o}/\lambda_{1o})DT} \quad (10)$$

In order to calculate reactivity ratio $r_v/(r_v)_o$ from equation 6, new dimensionless variables, SN and DN from equation 3 and 4 are introduced as follows:

$$SN = S_v/(2\varepsilon/R_m) = (\varepsilon_1/\varepsilon)\lambda_1 + (\varepsilon_2/\varepsilon)\lambda_2 \quad (11)$$

$$DN = D_e/(\varepsilon D_m/\tau) = (\varepsilon_1/\varepsilon) K_{r1} K_{p1} + (\varepsilon_2/\varepsilon) K_{r2} K_{p2} \quad (12)$$

Then,

$$\frac{r_v}{(r_v)_o} = \left(\frac{\varepsilon}{\varepsilon_o}\right)\left(\frac{SN\ DN}{SN_o\ DN_o}\right)^{1/2} \quad (13)$$

where SN_o and DN_o are initial values for SN and DN respectively. An equation for $\varepsilon/\varepsilon_o$ can be expressed in terms of the dimensionless varioable DT as follows:

$$\varepsilon/\varepsilon_o = \varepsilon_1/\varepsilon_o + \varepsilon_2/\varepsilon_o = (\varepsilon_{1o}/\varepsilon_o)(\varepsilon_1/\varepsilon_{1o}) + (\varepsilon_{2o}/\varepsilon_o)(\varepsilon_2/\varepsilon_{2o}) \quad (14)$$

In equation 14 each first term, i.e. $\varepsilon_{1o}/\varepsilon_o$ and $\varepsilon_{2o}/\varepsilon_o$ is given in the computer program as initial values. Also each second term can be rearranged as follows:

$$\frac{\varepsilon_1}{\varepsilon_{1o}} = \frac{R_1^2}{R_{1o}^2} = (1 - \delta/R_{1o})^2 = (1 - DT)^2 \quad (15)$$

$$\frac{\varepsilon_2}{\varepsilon_{2o}} = (1 - \delta/R_{2o})^2 = [1 - (\lambda_{2o}/\lambda_{1o})\,DT]^2 \quad (16)$$

Another porosity ratio $\varepsilon_2/\varepsilon$ in the calculation of SN and DN can be easily obtained using equations 14-16, that is,

$$\frac{\varepsilon_2}{\varepsilon} = \frac{\varepsilon_2/\varepsilon_o}{\varepsilon/\varepsilon_o} = \frac{(\varepsilon_{2o}/\varepsilon_o)(\varepsilon_2/\varepsilon_{2o})}{\varepsilon/\varepsilon_o} \quad (17)$$

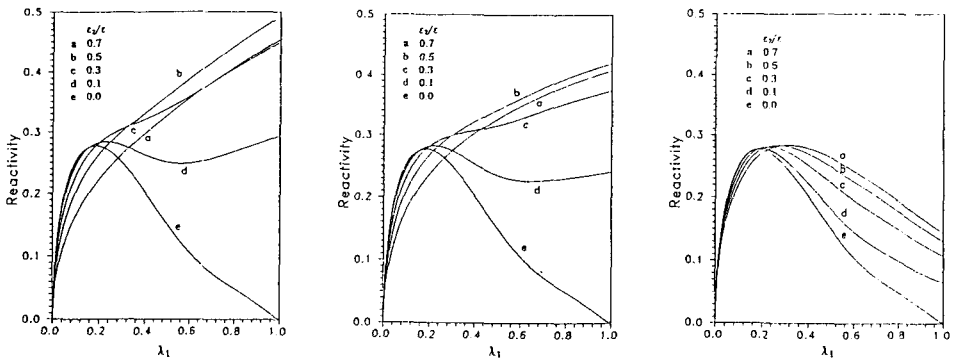

a) b) c)

Fig. 1. Reactivity vs. λ for Constant Total Porostiy
a) $\lambda_2/\lambda_1=0.01$
b) $\lambda_2/\lambda_1=0.1$
c) $\lambda_2/\lambda_1=0.5$

The surface area ratio, S_v/S_{vo} and diffusivity ratio, D_e/D_{eo} are obtained using the above equations as follows:

$$\frac{S_v}{S_{vo}}=\left(\frac{\varepsilon}{\varepsilon_o}\right)\left(\frac{SN}{SN_o}\right) \tag{18}$$

$$\frac{D_e}{D_{eo}}=\left(\frac{\varepsilon}{\varepsilon_o}\right)\left(\frac{DN}{DN_o}\right) \tag{19}$$

In case of a unimodal catalyst the macroporosity ε_2 equals zero and ε is equat to ε_1. Thus the following relations exist. The subscript u represents a unimodal catalyst.

$$SN|_u=\lambda_1 \tag{20}$$

$$DN|_u=K_{r1}K_{p1} \tag{21}$$

$$\left(\frac{r_v}{r_{vo}}\right)|_u=\left(\frac{\varepsilon_1}{\varepsilon_{1o}}\right)\left(\frac{\lambda_1}{\lambda_{1o}}\right)^{1/2}\left(\frac{K_{r1}K_{p1}}{K_{r1o}K_{p1o}}\right) \tag{22}$$

$$\left(\frac{S_v}{S_{vo}}\right)|_u=\left(\frac{\varepsilon_1}{\varepsilon_{1o}}\right)\left(\frac{\lambda_1}{\varepsilon_{1o}}\right) \tag{23}$$

$$\left(\frac{D_e}{D_{eo}}\right)|_u=\left(\frac{\varepsilon_1}{\varepsilon_{1o}}\right)\left(\frac{K_{r1}K_{p1}}{K_{r1o}K_{p1o}}\right) \tag{24}$$

Equation 24 assumes that the tortuosity remains constant during deactivation.

Based on each initial value of the unimodal catalyst, the relative values of the bimodal catalyst for reactivity, surface area and diffusivity can be obtained as follows:

$$\frac{(r_v)|_b}{(r_{vo})|_u}=\left(\frac{\varepsilon}{\varepsilon_{1o}}\right)\left(\frac{SN\,DN}{\lambda_{1o}K_{r1o}K_{p1o}}\right)^{1/2} \tag{25}$$

$$\frac{(S_v)|_b}{(S_{vo})|_u}=\left(\frac{\varepsilon}{\varepsilon_{1o}}\right)\left(\frac{SN}{\lambda_{1o}}\right) \tag{26}$$

$$\frac{(D_e)|_b}{(D_{eo})|_u}=\left(\frac{\varepsilon}{\varepsilon_{1o}}\right)\left(\frac{DN}{K_{r1o}K_{p1o}}\right)^{1/2} \tag{27}$$

Here, the subscript b denotes a bimodal catalyst.

For simplicity the X-axis in the figures has been normalized to range from 0 to 1 using the following. From equation 8 and restriction for λ_1, i.e. $\lambda_{1o}\le\lambda_1\le1$, the restriction for DT becomes $0\le DT\le1-\lambda_{1o}$. A new variable DT′ is defined as follows:

$$DT'=DT/(1-\lambda_{1o}) \tag{28}$$

Thus, DT′ ranges from 0 to 1. $DT'=0$ means no coke buildup in the pores, and $DT'=1$ represents maximum coke buildup in the pores where the micropore size would be equal to the reactant molecular size.

3. Results and Discussion

3-1. Reaction Rate.

In order investigate the effects of macropores on the reactivity, the following two cases were studied by computer simulation.

Case 1. Constant Total porosity

Here the porosity $\varepsilon=\varepsilon_1+\varepsilon_2$ is assumed constant. For simplicity, the reactivity is defined as $r_v/(a'\varepsilon)$. Three typical plots of reactivity vs. λ_1 were obtained as

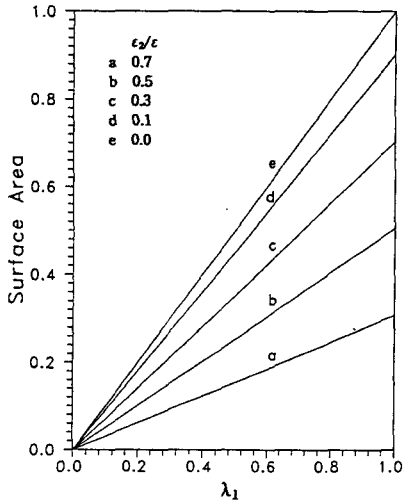

Fig. 2. Surface Area vs. λ_1 for Constant Total Porostiy ($\lambda_2/\lambda_1=0.01$)

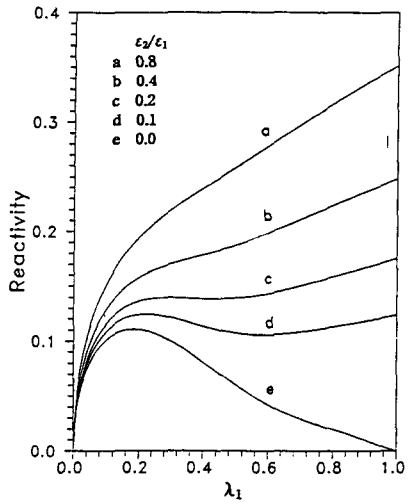

Fig. 4. Reactivity vs. λ_1 for Constant Microporosity ($\lambda_2/\lambda_1=0.01$, $\varepsilon_1=0.4$)

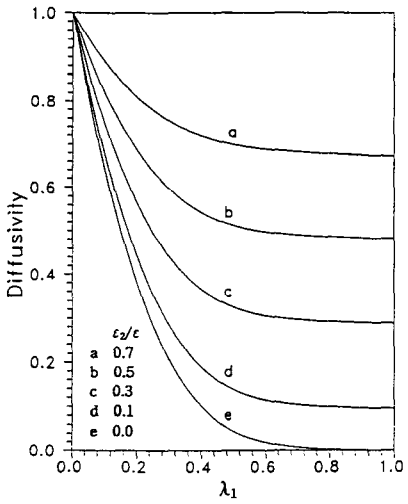

Fig. 3. Diffusivity vs. λ_1 for Constant Total Porostiy ($\lambda_2/\lambda_1=0.01$)

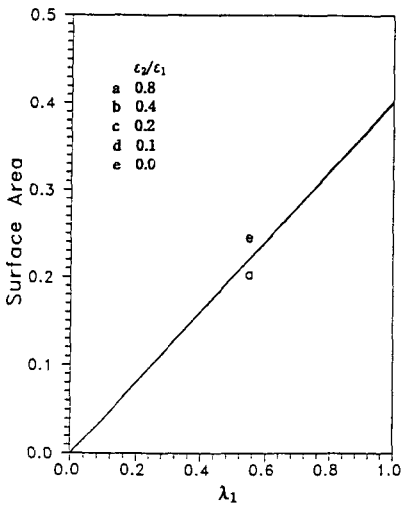

Fig. 5. Surface Area vs. λ_1 for Constant Microporosity ($\lambda_2/\lambda_1=0.01$, $\varepsilon_1=0.4$)

shown in Figure 1. In each plot four different ratios of macroporosity to total porosity $\varepsilon_2/\varepsilon$ were selected to investigate the effect of the macroporosity on the reactivity. In all plots, $\varepsilon_2/\varepsilon=0$ represents a unimodal catalyst. Also, a different value of λ_2/λ_1 is given in each plot. The smaller this value becomes, the greater the difference between the size of macropores and micropores becomes. λ_1 represents the ratio of reactant molecular size to micropore size. Thus $\lambda_1=0$ means that the micropore size goes to infinity, resulting in no reaction for both unimodal and bimodal catalyst. In case of $\lambda_1=1$, all micropores are inaccessible to reactant molecules, and no reaction occurs in the unimodal catalyst.

As shown in Figure 1, an optimal point exists and $\lambda_1=0.18$ for unimodal catalyst. This result may be useful for catalyst design where the reactivity is maximized. If the reactant molecule size were 20 angstroms in diameter, the optimal pore size would be 110 angstroms. The optimum results from the trade off

between surface area and diffusivity. In case of the bimodal catalyst, the existence of the optimal point depends on two model parameters, i.e. $\varepsilon_2/\varepsilon$ and λ_2/λ_1. Many combinations of these two model parameters for the existence of the optimal point are possible as can be seen in the three graphs. Mathematically, this phenomena can be considered as a transitional state from the bimodal catalyst to the unimodal catalyst. Do[13] and Ruckenstein and Tsai[14] reported similar observations in their modelling work.

Another interesting result is the existence of crossover in the reactivity. In other words, the activity of bimodal catalyst is below that of unimodal catalyst in some region of λ_1. This crossover also depends on the two model parameters. This result may come from the trade-off between catalytic surface area and effective diffusivity. As the size of molecules gets smaller, the effective diffusivity defined as $D_e/(D_m\,\varepsilon/\tau)$ in Figure 3 increases. However, as shown in Figure 2, the surface area defined as $S_v/(2\,\varepsilon/R_m)$ decreases with the introduction of macropores. Thus this dependence of two model parameters on λ_1 produces the crossover. This optimization problem, i.e. the problem of selecting either micropores or macropores from the viewpoint of surface area and diffusivity to obtain the highest reaction rate in a fixed pellet geometry has been reported in the literature.[13-15]

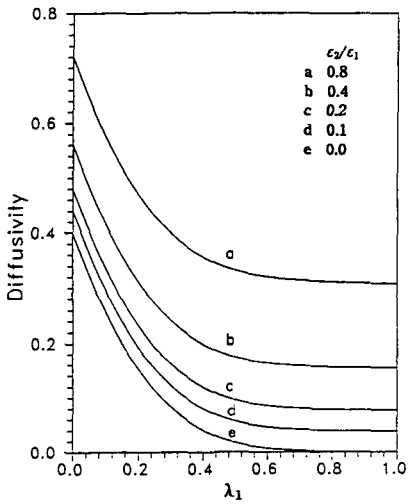

Fig. 6. Diffusivity vs. λ_1 for Constant Microporosity ($\lambda_2/\lambda_1=0.01$, $\varepsilon_1=0.4$)

Ruckenstein and Tsai[16] were able to obtain the optimum pore sizes $\lambda=0.52$ or 0.18 for reaction rate depending on the function $F(\lambda)$. In a fixed bed reactor the optimum pore size has been reported to depend on both physico-chemical characteristics of a reacting system and bulk concentration around catalyst pellets. [13] Delancey[15] reported that the optimum composition and density exist for pellets formed from single supports. Two parameters, i.e. Thiele modulus for the micro granule and interparticle voidage were found to affect the optimum density.

Case 2. Constant Mlicroporosity

In this case, the microporosity ε_1 is assumed constant when the macroporosity ε_2 is added to the unimodal catalyst to make a bimodal catalyst. In this case the total porosity ε will be increased according to the simple relation $\varepsilon=\varepsilon_1+\varepsilon_2$. The reactivity is defined as

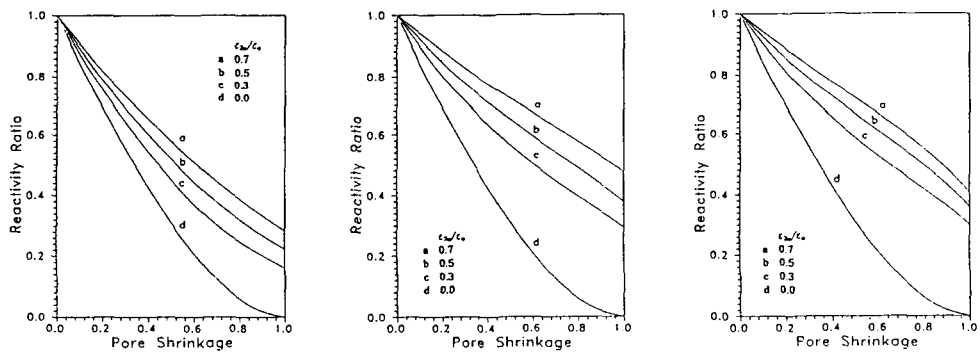

Fig. 7. Reactivity Ratio vs. Pore Shrinkage for $\lambda_{1o}=0.18$
a) $\lambda_{2o}/\lambda_{1o}=0.5$
b) $\lambda_{2o}/\lambda_{1o}=0.1$
c) $\lambda_{2o}/\lambda_{1o}=0.01$

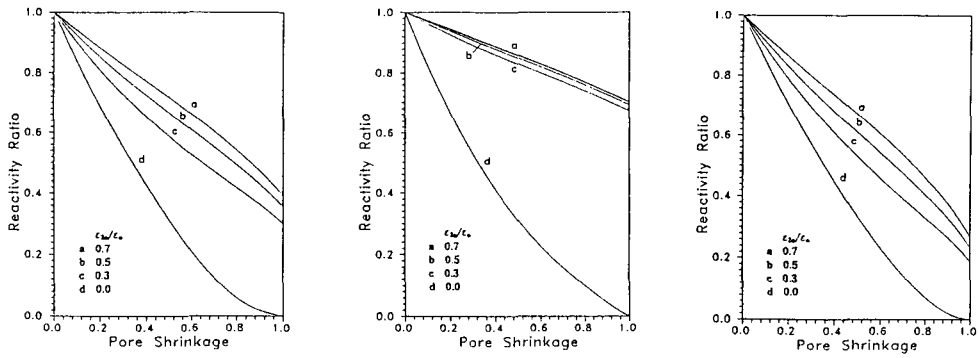

a) b) c)

Fig. 8. Reactivity Ratio vs. Pore Shrinkage for $\lambda_{2o}/\lambda_{1o}=0.001$
a) $\lambda_{2o}=0.18$
b) $\lambda_{2o}=0.5$
c) $\lambda_{2o}=0.09$

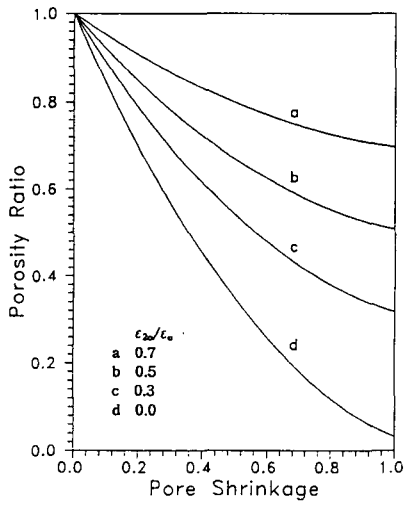

Fig. 9. Porosity Ratio vs. Pore Shrinkage
($\lambda_{1o}=0.18$, $\lambda_{2o}/\lambda_{1o}=0.01$)

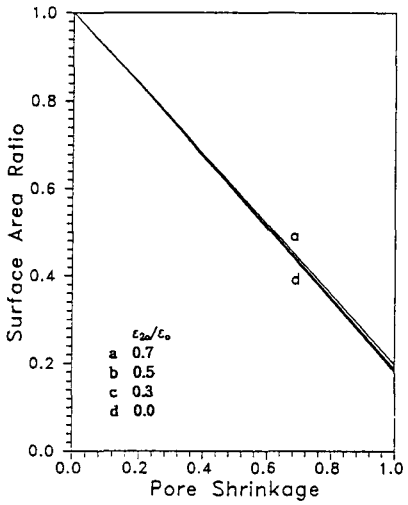

Fig. 10. Surface Area Ratio vs. Pore Shrinkage
($\lambda_{1o}=0.18$, $\lambda_{2o}/\lambda_{1o}=0.01$)

r_v/a'

Compared to the results of case 1, the graph of reactivity vs. λ_1 does not show any crossover as shown in Figure 4. This is not a surprising result if we consider that the catalyltic surface area defined as $S_v/(2/R_m)$ in Figure 5 mostly depends on the microporosity rather than the macroporosity. As shown in Figure 5, addition of the macroporosity will not contribute significantly to an increase of the surface area. Instead it will help reactant molecules diffuse into the pores as shown in Figure 6, where the diffusivity is defined as $D_e/(D_m/\tau)$. Eventually the reaction of the bimodal catalyst will result in higher performance than that of the unimodal catalyst.

3-2. Catalyst Deactivation.

Using equations 11 and 22 the reactivity ratio was calculated in terms of pore shrinkage defined as DT'. Initial values for λ_1, λ_2/λ_1, and $\varepsilon_2/\varepsilon$ were systematically selected to investigate the effects of each model parameter on catalyst deactivation. Figure 7 shows that a bimodal catalyst having more macropore volume has less decline in reactivity having more macropore volume has less decline in reactivity ratio with increasing $\lambda_{2o}/\lambda_{1o}$ for $\lambda_{1o}=0.18$. However, the effect of $\lambda_{2o}/\lambda_{1o}$ levels off when its value becomes small as can be seen in Figures 7-c and 8-a. This result indicates that

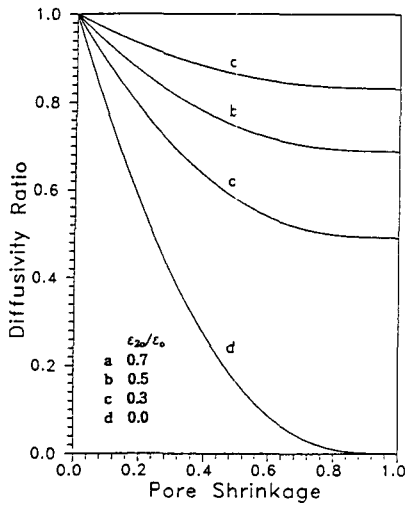

Fig. 11. Diffusivity Ratio vs. Pore Shrinkage ($\lambda_{1o}=0.18$, $\lambda_{2o}/\lambda_{1o}=0.01$)

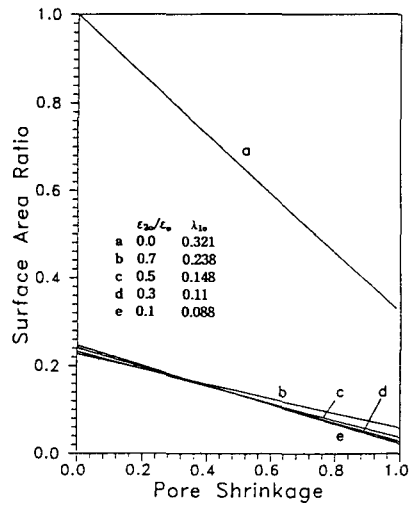

Fig. 13. Surface Area Ratio vs. Pore Shrinkage ($\varepsilon_{1o}=0.5$, $\lambda_{2o}/\lambda_{1o}=0.01$)

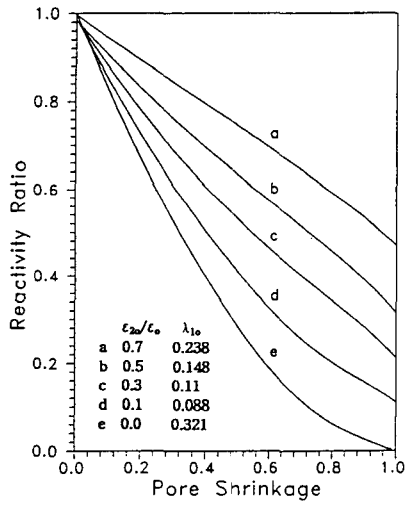

Fig. 12. Reactivity Ratio vs. Pore Shrinkage ($\varepsilon_{1o}=0.5$, $\lambda_{2o}/\lambda_{1o}=0.01$)

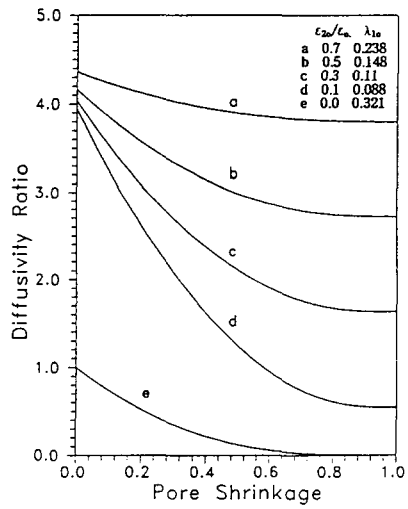

Fig. 14. Diffusivity Ratio vs. Pore Shrinkage ($\varepsilon_{1o}=0.5$, $\lambda_{2o}/\lambda_{1o}=0.01$)

the macropores can play a significant role in catalyst deactivation by reducing pore plugging. One reason why a bimodal catalyst has better performance during deactivation than the unimodal catalyst can be seen using the results of Figures 9-11. With an increase of $\varepsilon_{2o}/\varepsilon_o$, the reduction of the diffusivity ratio D_e/D_{eo} becomes much slower whereas the differences in the change of the surface area ratio S_v/S_{vo} are negligible. Eventually the combined result of the two parameters gives better performance for the bimodal catalyst.

The effects of λ_{1o} at $\lambda_{2o}/\lambda_{1o}=0.001$ were investigated as shown in Figure 8. With an increase of λ_{10} the reactivity ratios of bimodal catalysts approach each other, and tend toward straight lines. In other words, dimensionless micropore size does not affect the deactivation of bimodal catalysts greatly if λ_2/λ_{1o} is large enough. Also, the reduction of the porosity ratio $\varepsilon/\varepsilon_o$ that directly affects the reduction of the reactivity ratio is similar to that of D_e/D_{eo} as shown in Figure 9.

Based on each initial state of the unimodal catalyst,

the reactivity, surface area, and diffusivity ratios were calculated using equations 25-27. Several model parameters such as ε_o, $\lambda_{2o}/\lambda_{1o}$, $\varepsilon_{2o}/\varepsilon_{1o}$ and λ_{1o} were selected to produce the same initial reactivity of 0.24 in Figure 1. The result shown in Figure 12 can be used to directly compare the effect of macroporosity on catalyst deactivation because the reactivity ratios are obtained on the basis of the same initial reactivity of the unimodal catalyst. Figure 12 clearly shows that the bimodal catalyst has advantages with regard to catalyst deactivation compared to the unimodal catalyst.

The catalyst having the larger macroporosity becomes less deactivated even if the initial reactivities of the two catalysts are same. This behavior can be explained using the results of Figures 13 and 14. At the same initial reactivity, the unimodal catalyst has higher initial surface area and lower diffusivity as compared to bimodal catalysts. If it is noticed that the multiplication of surface area ratio and diffusivity ratio gives the reactivity ratio, the results shown in Figure 16 can be understood from the behavior of surface area and diffusivity shown in Figures 13 and 14. Thus, under the assumption of uniform coke buildup, the bimodal catalyst appears to offer improved resistance to deactivation as contrasted to its unimodal counterpart.

Conclusion

The optimal point observed in the constant total porosity system may be applied to catalyst design to maximize the reactivity. The significance of optimizing catalyst pore structure was demonstrated by the existence of crossover which could be explained in terms of catalyst surface area and effective diffusivity.

In the constant microporosity system, the introduction of macropores resulted in improved reactivity and the crossover effect was not observed.

In the catalyst deactivation where uniform coke buildup was assumed, a bimodal catalyst gave higher performance than a unimodal catalyst. Aunimodal catalyst with large pores provided much more improved resistance than that with small pores.

The results shown by this model hold promise for the development of improved catalysts for coprocessing and coal liquefaction.

Nomenclature

A : Cross sectional area of a pore, cm^2
a : Constant defined in equation 5
a' : Constant defined in equation 6
C : Solute concentration based on total pore volume, mole/*l*
D_e : Effective diffusivity, cm^2/s
D_m : Molecular bulk diffusivity, cm^2/s
DN : Dimensionless variable defined in equation 12
DT : Dimensionless coating thickness defined in equation 9
DT' : Dimensionless coating thickness defined in equation 28
F : Combined function of K_r and K_p
g : Pore size distribution function
K_p : Steric coefficient
K_r : Frictional drag coefficient
k : Overall reaction rate constant, s^{-1}
k_s : Surface reaction rate constant, cm/s
N : Number of pores
R : Average pore radius, cm
R_m : Size of diffusing species, cm
r_v : Reaction rate based on pellet volume, mole/cc-s
S_g : Surface area per unit pellet weight, cm^2/g
S_v : Surface area per unit pellet volume, cm^{-1}
S_x : Characteristic surface area of pellet, cm^2/g
SN : Dimensionless variable defined in equation 11
t : Time, s
V_p : Characteristic pellet volume, cc/g

Greek Letters

δ : Coating thickness in catalyst deactivation, angstroms
ε : Porosity
λ : Ratio of molecule radius to pore radius
ρ_c : Pellet density (apparent density), g/cc
ρ_s : Solid density (true density), g/cc
τ : Tortuosity

Subscripts

1 : for micropores
2 : for macropores
b : for bimodal catalyst
i : for componetn i
o : for initial values at t=0
u : for for unimodal catalysts

References

1. Ho, P.N. and Weller, S.W.: *Fuel Processing Tech-*

nol., **4**, 21 (1981).
2. Ternan, M.: *Can. J. Chem. Eng.*, **61**, 689 (1983).
3. Hardin, A.H., Packwood, R.H., and Ternan, W.: *Preprints, Div. Petroleum Chem., Amer. Chem. Soc.*, **23(4)**, 1450 (1978).
4. Hardin, A.H. and Ternan, M.: *Preprints, 2nd World Congress on chemical Engineering*, **3**, 134 (1981).
5. Yen, Y.K., Furlani, D.E., and Weller, S.W.: *Ind. Eng. Chem. Production Research and Development*, **15(1)**, 24 (1976).
6. Shimada, H., Kurita, M., Sato, T., Yoshimura, Y., Kobayashi, Y., and Nishijima, A.: *Bull. Chem. Soc. Jpn.*, **59**, 2885 (1986).
7. Shimura, M., Shiroto, Y., and Takeuchi, C.: *Ind. Eng. Chem. Fundam.*, **25**, 330 (1986).
8. Curtis, C.W., Guin, J.A., Kamajina, B.L., and Moody, T.E.: *Fuel Processing Technol.*, **12**, 111 (1986).
9. Spry, J.C. and Sawyer, W.H.: "Configurational Diffusion Effects in Catalytic Demetallization of Petroleum Feedstocks", Presented at 68th Annual AIChE Meeting, LA, CA (Nov. 1975).
10. Tischer, R.E., Narain, N.K., Stiegel, G.J., and Cillo, D.L.: *J. Cat.*, **95**, 406 (1985).
11. Nalitham, R.V., Lee, J.M., Lamb, C.W., and Johnson, T.W.: *Fuel Processing Technol.*, **17**, 13 (1987).
12. Rhee, Y.W. and Guin, J.A.: *KJChE*, **10(1)**, 56 (1993).
13. Do, D.D.: *AIChE J.*, **30**, 849 (1984).
14. Ruckenstein, E. and Tsai, M.C.: *AIChE J.*, **27**, 697 (1981).
15. De Lancey, G.B.: *Chem. Eng. Sci.*, **29**, 1391 (1974).
16. Baltus, R.E. and Anderson, J.L.: *Chem. Eng. Sci.*, **38(12)**, 1959 (1983).